p. ISSN: 2354-9610, e. ISSN:2614-5081

IJCR – INDONESIAN JOURNAL OF CHEMICAL

Vol. 11, No. 1, Hal. 104-120 (July 2026)

Photocatalytic Performance and Greenness Analysis of Magnetic Biochar Prepared from Banana (Musa acuminata) Peel Waste

Analisis Aspek Keberlanjutan Lingkungan (Greenness Analysis) Biochar Magnetik yang Disintesis dari Limbah Kulit Pisang (*Musa acuminata*)

Indah Tri Rizky[1], Nunung Nurlaela[1], Azlan Kamari[2], Suresh Sagadevan[3], and Is Fatimah[1*]

[1]Chemistry Department, Universitas Islam Indonesia, Yogyakarta, 55581, Jl. Kaliurang Km 14, Sleman, Yogyakarta, Indonesia, 55584.
[2]Chemistry Department, Faculty of Sciences and Mathematics, Universiti Pendidikan Sultan Idris, Tanjong Malim, Perak, Malaysia
[3]Institute of Analytical and Environmental Sciences, National Tsing Hua University, 101, Section 2, Kuang Fu Road, Hsinchu 30013, Taiwan

[*]Corresponding author: isfatimah@uii.ac.id

Submitted: 07 May 2026, Revised: 02 July 2026, Accepted: 07 July 2026

ABSTRACT

Magnetic biochar was prepared from Kepok banana (Musa acuminata) peel and evaluated as a photocatalyst for the degradation of Rhodamine B in aqueous solution. The material was synthesized by impregnating an iron precursor onto the biochar, followed by pyrolysis at 600 °C for 2 h. The prepared material was characterized by X-ray diffraction (XRD), Fourier-transform infrared (FTIR) spectroscopy, and vibrating-sample magnetometry (VSM). The analyses revealed the formation of dispersed iron oxide within the carbonaceous biochar structure, with a saturation magnetization of 1.91 emu g^{-1}*. The magnetic biochar exhibited pronounced photocatalytic activity toward Rhodamine B degradation, achieving an optimum efficiency of 98.85%. The greenness of the preparation method was assessed using the AGREE platform, which yielded a score of 0.73, indicating good compliance with the principles of green chemistry. These results demonstrate that banana peel-derived magnetic biochar is a promising, environmentally friendly material for the treatment of dye-containing wastewater.*

Keywords: Biochar; Magnetic Biochar; Photocatalysis; Green Chemistry.

ABSTRAK

Pada penelitian ini dilakukan preprasi biochar magnetic dari pisang Kepok (*Musa acuminata)*. Material dikembangkan sebagai fotokatalis pada degradasi rhodamine B. Sintesis dilakukan dengan cara impregnasi precursor besi pada biochar dilanjutkan pirolisis pada 600°C selama 2 jam. Karakterisasi material dilakukan menggunakan XRD, FTIR dan VSM. Analisis instrumental membuktikan terdispersinya oksida logam pada struktur karbon biochar dengan magnetisasi 1.91 emu. g^{-1}. Material menunjukkan sifat fotoaktif dengan efisiensi degradasi sebesar 98.85%. Analisis keramahlingkunganan material dilakukan dengan platform *AGREE* dan diperoleh skor 0.73, mengindikasikan kesesuaian dengan prinsip green chemistry. Hasil menunjukkan potensi biochar magnetic sebagai material pada pengolahan limbah cair mengandung zat warna.

Kata-kata kunci: Biochar; Biochar magnetik; Fotokatalisis; Green Chemistry.

INTRODUCTION

Dye effluents from the textile and batik industries are among the most persistent and hazardous sources of water pollution. The dyeing and washing of fabrics generate large volumes of wastewater containing synthetic dyes and auxiliary chemicals. Approximately 10–15% of the dyes fail to bind to the fabric fibers and are consequently lost to the effluent (Deviliana et al., 2019). The discharge of such colored effluent into water bodies disrupts aquatic ecosystems, reduces light penetration, and exerts toxic effects on both aquatic organisms and humans (Zakaria et al., 2023; Juliani et al., 2021).

Rhodamine B (RhB) is a widely used cationic dye that is frequently detected in textile effluents. Its stable and persistent aromatic structure renders it resistant to natural degradation. In addition, RhB is toxic, mutagenic, and carcinogenic, and it is therefore commonly employed as a model compound for evaluating material performance in dye wastewater treatment (Rafique et al., 2020). The use of model compounds such as RhB allows more controlled testing than real batik wastewater, which possesses a highly complex composition.

Conventional wastewater treatment methods, such as adsorption, coagulation, and biological processes, generally transfer dyes from the liquid phase to another phase without decomposing their molecular structures. Moreover, these methods often require large quantities of chemicals and generate sludge that can act as a secondary source of pollution (Rohayati et al., 2017; Haryono et al., 2018). Treatment technologies capable of degrading dyes at the molecular level are therefore required.

Advanced oxidation processes (AOPs) are effective strategies for decomposing persistent organic compounds, as they generate reactive species such as hydroxyl radicals (•OH), superoxide radicals ($O_2^{\bullet-}$), and hydroperoxyl radicals ($HO_2^{\bullet}$) that oxidize dye molecules into simpler and less harmful products (Priyadarshini et al., 2022). Among the AOPs, photo-oxidation is widely adopted; it employs light energy, specifically ultraviolet (UV) radiation, to activate catalysts and accelerate the generation of reactive radicals (Frankel, 2012; Irwan et al., 2023).

The efficiency of the photo-oxidation process is strongly influenced by the type of catalyst employed. Biomass-derived biochar (BC) is an attractive candidate owing to its low cost, porosity, and environmental compatibility. Biochar bears oxygenated functional groups, such as –OH and –COOH, that act as active sites for adsorption and catalytic reactions (Xie et al., 2022). Modification of biochar with metal oxides, particularly Fe_2O_3, can enhance its catalytic activity and enable magnetic separation under an external field, yielding magnetic biochar (MBC) (Navarathna et al., 2020). This magnetic character increases the practicality of the material for wastewater treatment applications (Li et al., 2021; Fatimah et al., 2022).

Banana peels constitute an abundant agricultural waste whose valorization remains limited. Chemically, they are a lignocellulosic biomass rich in cellulose, hemicellulose, pectin, and lignin, which enables the production of biochar with a stable and porous structure (Kumar Mishra et al., 2023). Among the available varieties, Kepok banana (*Musa acuminata*) peels have a relatively thick texture and are widely available in Indonesia, making them a promising and sustainable feedstock for biochar synthesis. Nevertheless, the use of Kepok banana peels as a precursor for magnetic biochar in RhB degradation has not yet been extensively explored.

Beyond effectiveness, modern analytical and wastewater treatment methods are increasingly expected to comply with sustainability principles. Green analytical chemistry emphasizes the reduction of hazardous substances, low energy consumption, and waste minimization across all stages of a method. The Analytical Greenness Calculator (AGREE) was developed to evaluate the greenness of a method against the twelve principles of green analytical chemistry (Pena-pereira et al., 2020). Assessment with AGREE is therefore valuable for determining whether a photocatalytic system is both effective and environmentally benign.

Accordingly, the present study aims to develop a green photocatalytic system based on magnetic biochar derived from Kepok banana peels for the degradation of RhB. The synthesized material was characterized to confirm the formation of a magnetically active phase and to evaluate its physicochemical properties, and was subsequently applied to the photo-oxidation of RhB in the presence of H_2O_2 under UV irradiation. In addition, the sustainability of the synthesis, characterization, and application steps was assessed using AGREE to provide a comprehensive overview of the environmental performance of the system.

MATERIALS AND METHODS

2.1. Materials and Instrumentation

Kepok banana peels (*Musa acuminata*) were collected from a traditional market in Sleman District, Indonesia. Iron(III) chloride hexahydrate ($FeCl_3\cdot6H_2O$), hydrogen peroxide (H_2O_2), and RhB were of analytical grade, purchased from Merck, and used without further purification. Ultra-high-purity (UHP) N_2 gas was supplied by Samator Indonesia.

The main instruments comprised a pyrolysis reactor equipped with a tubular furnace and a temperature controller, a HITACHI U-2080 UV–Vis spectrophotometer, a Shimadzu X6000 X-ray diffractometer (XRD), a Perkin Elmer Fourier-transform infrared (FTIR) spectrometer, a vibrating-sample magnetometer (VSM), a scanning electron microscope (SEM; JEOL), and a transmission electron microscope (TEM; JEOL).

2.2. Synthesis of Biochar from Kepok Banana Peels

Kepok banana peels were thoroughly washed with distilled water to remove surface impurities, sun-dried, and subsequently oven-dried at 100 °C to constant weight. The dried peels were cut into small pieces, and 25 g was placed in the pyrolysis reactor. Pyrolysis was carried out at 600 °C for 2 h under a nitrogen (N_2) atmosphere to yield biochar (BC).

2.3. Magnetic Biochar Synthesis

Twenty-five grams of dried banana peels were immersed in an iron precursor solution prepared by dissolving 50 g of $FeCl_3 \cdot 6H_2O$ in 250 mL of distilled water. The suspension was stirred magnetically for 12 h at room temperature to ensure effective impregnation of the iron precursor into the peels. The mixture was then oven-dried at 105 °C until a dry solid was obtained. Finally, the solid was pyrolyzed at 600 °C for 2 h under a nitrogen atmosphere to afford magnetic biochar (MBC).

2.4. Material Characterization

The physicochemical properties of BC and MBC were characterized using several complementary techniques. The crystal structure and phase composition were determined by XRD, and the surface functional groups were identified by FTIR spectroscopy. The magnetic properties were evaluated by VSM, whereas SEM was used to examine the morphology and the distribution of Fe particles. TEM was employed to assess the particle size and nanostructure.

2.5. Photocatalytic Activity

The photocatalytic activity toward RhB degradation was evaluated using BC and MBC as catalysts. In a typical experiment, 250 mL of RhB solution (20 ppm) was transferred to the reactor, followed by the addition of 0.5 g of catalyst (BC or MBC) and 0.5 mL of H_2O_2. The mixture was stirred and irradiated with UV light. At predetermined time intervals, aliquots of approximately 5 mL were withdrawn and analyzed with a UV–Vis spectrophotometer at 554 nm.

In additional experiments, a 40 ppm

RhB solution was treated with 0.5 g of MBC. The volume of H_2O_2 was varied (0.03, 0.05, and 0.1 mL) to examine its influence on the photocatalytic degradation. The reactions were performed under identical conditions, and the change in RhB concentration was monitored spectrophotometrically.

The degradation efficiency (DE) was calculated using the following equation:

$$DE(\%) = \frac{C_0 - C_t}{C_0} x100\%$$

where C_0 and C_t denote the initial concentration and the concentration at time t, respectively.

2.6. Green Analytical Chemistry Evaluation

The sustainability of the synthesis, characterization, and photocatalytic application was evaluated using the Analytical Greenness Calculator (AGREE) (Pena-pereira et al., 2020; Ozkan et al., 2025). The AGREE score was computed from the twelve principles of green analytical chemistry to assess the environmental impact of the developed method.

3. Results and Discussion

3.1. Synthesis and Characterization of Magnetic Biochar

The synthesis of magnetic biochar is based on the use of the carbonaceous biochar as a support for photocatalytically active Fe_2O_3. Figure 1 illustrates the synthesis scheme and the proposed structure of the material.

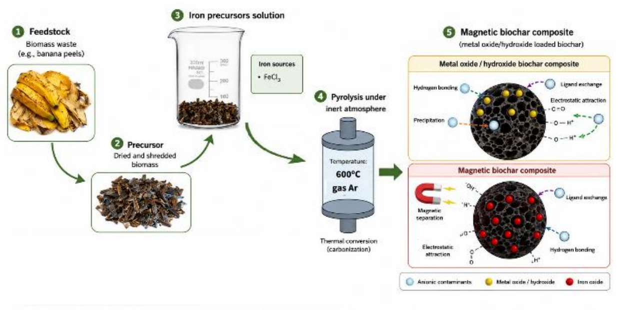

Figure 1. Scheme of Procedure and MBC structure

The formation of iron oxide in the MBC was confirmed by XRD analysis, and the corresponding patterns are presented in Figure 2.

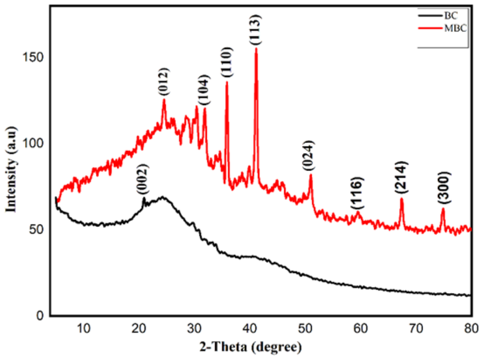

Figure 2. XRD pattern of materials

The diffractogram of BC exhibits a single broad reflection at 2θ ≈ 20.9°, assigned to the (002) plane of amorphous carbon, which is characteristic of biochar derived from lignocellulosic biomass. The absence of sharp reflections indicates that BC is dominated by an amorphous carbon phase, with no significant crystalline mineral phases.

In contrast, the MBC pattern displays several sharp reflections at 2θ ≈ 24.53°, 31.88°, 35.87°, 41.14°, 50.92°, 59.45°, 67.33°, and 74.83°, corresponding to the (012), (104), (110), (113), (024), (116), (214), and (300) planes of the α-Fe_2O_3 (hematite) phase, respectively, in agreement with JCPDS card No. 33-0664 (Hussain et al., 2016). No diffraction peaks corresponding to other phases were detected, confirming the formation of single-phase hematite without additional iron oxide impurities.

The crystallite size of the α-Fe_2O_3 phase, estimated from the Scherrer equation, was 18.35 nm, indicating that the iron oxide is nanocrystalline. This small crystallite size is attributed to the porous biochar matrix, which restricts crystal growth and suppresses excessive agglomeration during pyrolysis.

The FTIR spectra of BC and MBC are shown in Figure 3. Both materials display bands at approximately 2100–2200 cm^{-1}, associated with C=O groups, which are further supported by the band at 790–795 cm^{-1}. The peaks at approximately 1590–1595 cm^{-1} indicate C=C stretching of the aromatic carbonaceous framework. The main difference between BC and MBC is that the strong absorption at 1052 cm^{-1} in BC shifts to 1054 cm^{-1} in MBC, which is interpreted as the formation of bonds between carbon and the incorporated metal that raise the vibrational energy. This assignment is corroborated by the peaks at 529 cm^{-1} and around 400 cm^{-1}, which correspond to metal–oxygen (Fe–O) bonding (Elnour et al., 2019; Reza et al., 2020).

The morphology and Fe distribution of MBC were examined by SEM–EDX (Figure 4). After modification, the biochar surface becomes rougher and is covered with small iron oxide particles.

The TEM image of MBC (Figure 5) reveals iron oxide nanoparticles dispersed within the carbon matrix, with an average particle size of approximately 82.54 nm. The nanoparticles are anchored on the surface and in the pores of the biochar, consistent with the XRD results indicating the formation of a nanocrystalline α-Fe_2O_3 phase. The slight agglomeration observed can be ascribed to magnetostatic interactions between particles, which are commonly encountered in iron oxide-based materials.

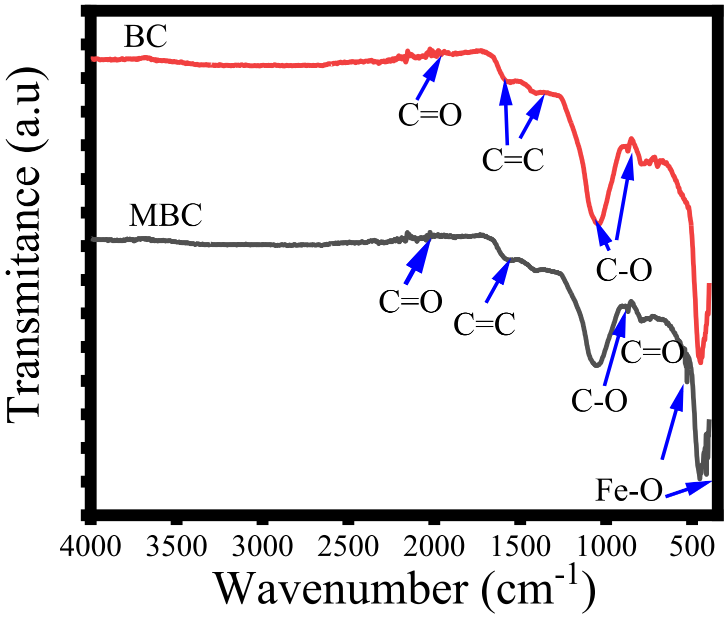

Figure 3. FTIR spectra of BC and MBC

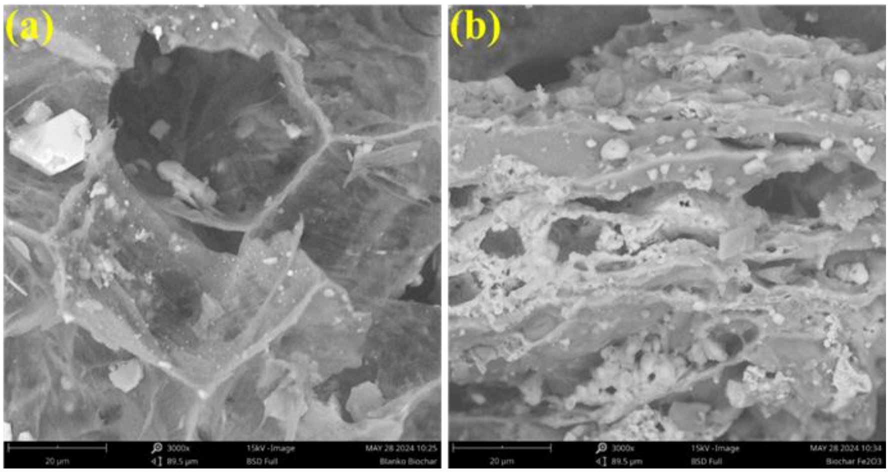

Figure 4. SEM of (a) BC and (b) MBC

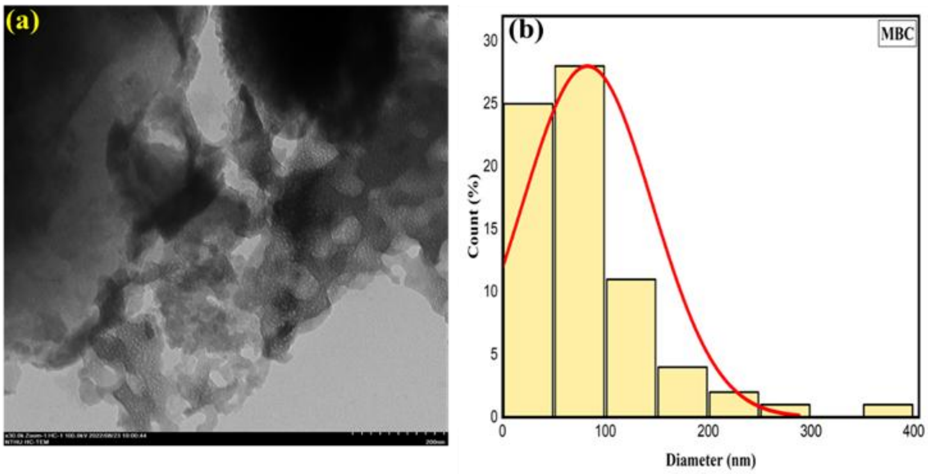

Figure 5. (a) MBC morphology, (b) MBC particle size histogram

3.2. Structural and Magnetic Properties of the Material

The structural and magnetic properties of MBC largely govern its photocatalytic performance and the ease with which it can be separated after the reaction. The crystallite size, particle size, and magnetic behavior were therefore analyzed to relate the material structure to its photocatalytic activity. The crystallite size of α-Fe_2O_3 in MBC, calculated from the XRD data using the Scherrer equation, was 18.35 nm, confirming the nanocrystalline nature of the iron oxide phase. Such a small crystallite size implies a relatively high specific surface area and a greater number of active sites, which may enhance the generation of reactive species during photocatalysis. Moreover, the porous biochar matrix acts as a support that restricts the growth of Fe_2O_3 crystals during pyrolysis, thereby preventing the formation of large particles and preserving their nanoscale dimensions.

The magnetic properties of MBC, evaluated by VSM, are characterized by a saturation magnetization of 1.91 emu g^{-1}, confirming that the material is ferromagnetic and can be readily separated under an external magnetic field (Figure 6). This value is comparable to that reported for a similar biochar/Fe_2O_3 composite prepared with an Alfa Aesar precursor (Zhang et al., 2019). It is lower than the saturation magnetization of pure iron oxide, owing to the presence of the carbonaceous matrix. The magnetization depends on several factors, including the iron oxide content and the particle size (Damertey et al., 2020). Nevertheless, it is sufficient for the rapid magnetic separation of the catalyst from solution after degradation, thereby supporting the objectives of sustainability and material reuse.

The combination of a small crystallite size, good nanoparticle dispersion within the biochar matrix, and appreciable magnetic properties confer synergistic advantages for photocatalytic applications. The nanocrystalline α-Fe_2O_3 provides active sites for the generation of electron–hole pairs under UV irradiation, while the porous biochar promotes the adsorption of RhB molecules in the vicinity of these sites. In addition, the magnetic separability of MBC obviates the need for filtration or centrifugation, thereby lowering energy consumption and reinforcing the green chemistry credentials of the developed system.

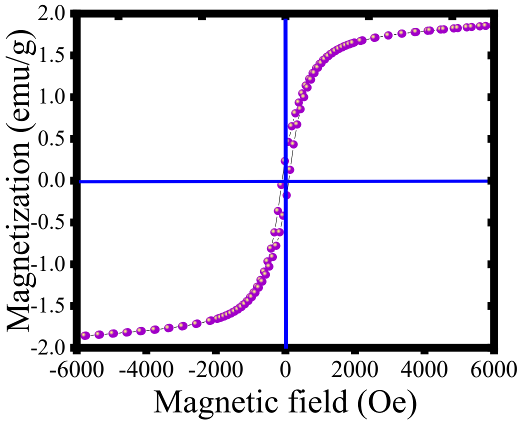

Figure 6. MBC Curve Hysteresis

Overall, these characterization results demonstrate that the Kepok banana peel-based magnetic biochar was successfully synthesized, comprising a nanocrystalline α-Fe_2O_3 phase dispersed within a carbon matrix and possessing the magnetic properties required for convenient separation.

3.3. Photocatalytic Activity of BC and MBC in Rhodamine B Degradation

The photocatalytic activity of BC and MBC was evaluated using a Rhodamine B (RhB) solution with an initial concentration of 20 ppm under UV irradiation in the presence of H_2O_2. The RhB concentration was monitored throughout the reaction with a UV–Vis spectrophotometer at 554 nm.

The RhB degradation profiles of BC and MBC are presented in Figure 7a. Both materials exhibited very high RhB removal from solution: BC degraded 99.01% of the RhB, while MBC reached 99.17%. Although MBC performed slightly better, the difference in the final degradation efficiency between the two materials was relatively small.

This small difference can be attributed to the relatively low initial RhB concentration (20 ppm). Under these conditions, the number of RhB molecules is limited relative to the adsorption and active sites available on the BC and MBC surfaces, so that almost all of the RhB can be adsorbed and degraded even by unmodified BC. Once most of the dye has been removed, too few molecules remain to reveal a clear performance difference between BC and MBC. The system thus operates under catalyst-rich conditions, and the contribution of the Fe_2O_3 phase is not fully expressed at low RhB concentrations.

Nevertheless, MBC still exhibits a

higher degradation rate than BC during the initial stage of the reaction, indicating that the α-Fe_2O_3 phase accelerates the formation of reactive species. This suggests that the primary role of Fe_2O_3 lies in the reaction kinetics rather than in the final degradation efficiency.

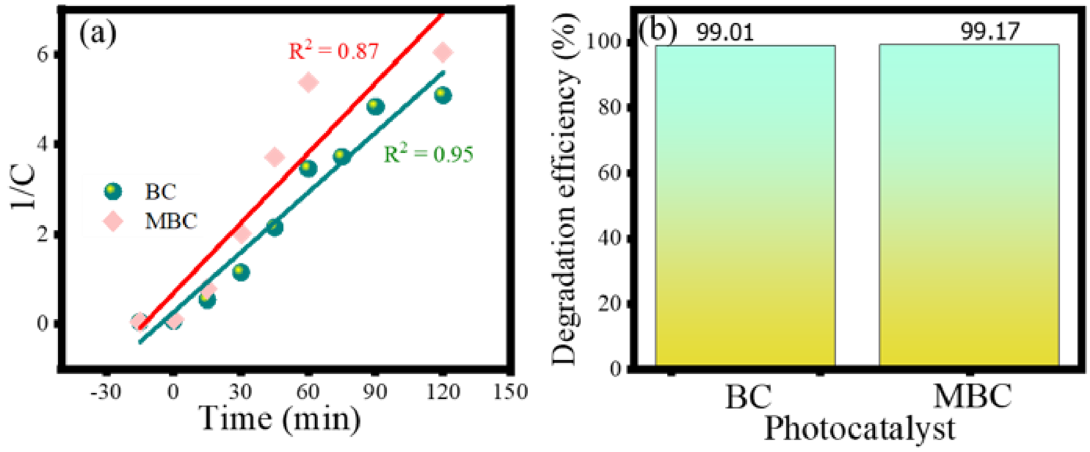

Figure 7. (a) RhB degradation profiles and (b) pseudo-second-order kinetic plots for BC and MBC.

3.4. Kinetics of the Photocatalytic Reaction

The photocatalytic behavior of the materials was analyzed using a kinetic model. A pseudo-second-order model was applied, as expressed by the following equation:

$$\frac{1}{C_t} - \frac{1}{C_0} = kt$$

where C_0 is the initial RhB concentration, C_t is the RhB concentration at time t, and k is the pseudo-second-order rate constant. Plots of *1/C* versus time for BC and MBC are shown in Figure 7b. Both systems exhibit good linearity, indicating that RhB degradation follows pseudo-second-order kinetics. However, the slope of the line for MBC is greater than that for BC, demonstrating that MBC has a higher reaction rate constant.

The higher rate constant of MBC indicates that the α-Fe_2O_3 phase accelerates the RhB degradation. Although the final degradation efficiencies of BC and MBC are almost identical at an initial concentration of 20 ppm, the kinetic analysis shows that MBC decomposes RhB more rapidly. This confirms that the principal difference between the two materials lies in the reaction rate rather than in the final removal efficiency.

The enhanced reaction rate of MBC is attributed to the role of Fe_2O_3 as a photocatalytically active phase that promotes the formation of reactive radicals under UV irradiation. Meanwhile, the porous biochar matrix acts as an adsorbent that increases the local concentration of RhB near the active sites, thereby accelerating the interaction between the dye molecules and the oxidative radicals. This synergy between biochar adsorption and Fe_2O_3 photocatalysis accounts for the superior degradation kinetics of MBC relative to BC.

3.5. Effect of H_2O_2 on RhB Degradation

To evaluate the performance of MBC under more demanding conditions, photocatalytic experiments were conducted using a RhB solution with an initial concentration of 40 ppm. The volume of H_2O_2 was also varied to probe the effect of oxidant availability on the degradation process. The resulting RhB degradation profiles under different H_2O_2 dosages are shown in Figure 8.

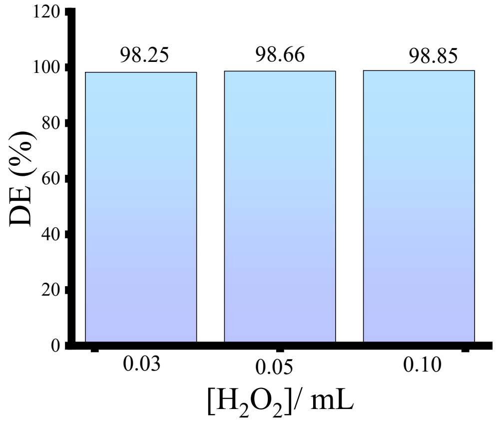

Figure 8. Effect of H_2O_2 on the degradation efficiency (DE, %).

The results indicate that the H_2O_2 dosage markedly influenced both the rate and the efficiency of degradation. At low H_2O_2 volumes, the amount of hydroxyl radicals (•OH) generated was limited, resulting in slower RhB degradation. Increasing the H_2O_2 volume promoted •OH formation and led to faster, more efficient RhB oxidation. At excessively high H_2O_2 volumes, however, the improvement in degradation efficiency became negligible. This behavior is ascribed to a radical-scavenging effect, whereby excess H_2O_2 reacts with •OH to form less reactive species such as HO_2•, thereby diminishing the oxidation of RhB.

The strong performance of MBC at higher RhB concentrations indicates that the α-Fe_2O_3 phase dispersed in the biochar matrix plays a crucial role in sustaining photocatalytic activity under elevated pollutant loads. The biochar concentrates RhB near the active sites, while Fe_2O_3

accelerates the formation of oxidative species under UV irradiation. This synergy allows MBC to remain effective even as the dye concentration increases.

3.6. Photocatalytic Mechanism

The degradation of RhB by MBC under UV irradiation in the presence of H_2O_2 involves a synergistic interaction between the α-Fe_2O_3 phase and the biochar matrix. Taking into account the band-gap energy of biochar-supported Fe_2O_3 reported previously as 2.6 eV (Elnour et al., 2019), a schematic representation of the reaction mechanism is shown in Figure 9.

Upon UV irradiation, the α-Fe_2O_3 particles absorb light and generate electron–hole pairs (e^-/h^+) at their surface. The photoexcited electrons are promoted from the valence band to the conduction band, where they react with dissolved oxygen or H_2O_2 to produce reactive species such as superoxide radicals ($O_2{\bullet}^-$) and hydroxyl radicals (•OH). Concurrently, the holes (h^+) oxidize water molecules or hydroxide ions (OH^-) to generate additional •OH. H_2O_2 serves as the principal source of hydroxyl radicals in this system: under UV irradiation and in the presence of Fe_2O_3, each H_2O_2 molecule decomposes into two highly oxidizing •OH radicals. These radicals attack the aromatic framework of RhB, cleaving the chromophoric bonds and oxidizing the dye into simpler intermediates that are ultimately mineralized to CO_2, H_2O, and inorganic ions.

The porous biochar matrix acts as an adsorbent that concentrates RhB molecules around the α-Fe_2O_3 surface. The resulting increase in the local RhB concentration near the active sites raises the probability of interaction between the dye and the reactive radicals, thereby enhancing the degradation rate. In addition, surface functional groups of the biochar, such as –OH and $-COO^-$, facilitate electron transfer and improve the stability of the iron oxide particles within the carbon matrix (Navarathna et al., 2020; Alharbi et al., 2023). The synergy between the photocatalytic activity of α-Fe_2O_3 and the adsorption capacity of the biochar accounts for the high performance of MBC in RhB degradation and explains its faster kinetics relative to unmodified biochar, as discussed above.

3.7. Evaluation of Green Analytical Chemistry Using AGREE

The greenness of the magnetic biochar-based photocatalytic system was evaluated using the Analytical Greenness Calculator (AGREE), which assesses analytical methods against the twelve principles of green analytical chemistry. The resulting AGREE score and its corresponding pictogram are shown in Figure 10.

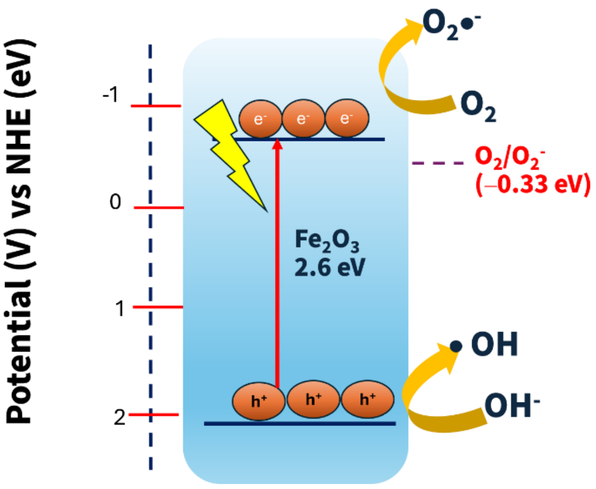

Figure 9. Photocatalytic reaction mechanism.

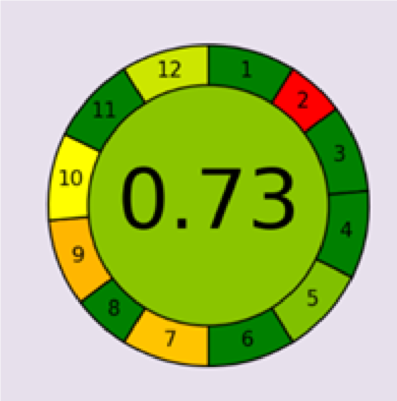

Figure 10. AGREE assessment score.

The overall AGREE score was 0.73, indicating a good level of sustainability for the developed method (Figure 10). This value reflects the environmentally friendly character of all stages of the method, from material synthesis and characterization to photocatalytic application. The use of banana peels as the biochar feedstock contributes markedly to resource sustainability, as it valorizes an abundant, low-value biomass waste.

The RhB degradation was performed under UV irradiation with the addition of only a small amount of H_2O_2, which decomposes into H_2O and O_2 after the reaction, leaving no harmful residues. Moreover, monitoring the RhB concentration by UV–Vis spectrophotometry is consistent with the principles of green analytical chemistry, as it requires no additional reagents, is non-destructive, and consumes relatively little energy.

A further advantage of the system is the magnetic character of MBC, which enables rapid and straightforward catalyst separation with an external magnet, without filtration or centrifugation. This feature reduces solvent use, energy consumption, and secondary waste generation, further enhancing the sustainability of the method.

Overall, the AGREE evaluation

confirms that the magnetic biochar-based photocatalytic system is not only effective for degrading RhB but also complies with the key principles of green analytical chemistry. This combination of high performance and sustainability underscores the strong potential of the developed method as an environmentally friendly approach for dye wastewater treatment.

CONCLUSIONS

A magnetic biochar was successfully synthesized from Kepok banana (*Musa acuminata*) peel waste and applied as a green photocatalytic system for the degradation of Rhodamine B. Characterization confirmed the formation of a nanocrystalline α-Fe_2O_3 phase dispersed within the biochar matrix, which imparted a saturation magnetization of 1.91 emu g^{-1} and thus enabled convenient magnetic separation of the catalyst. Under UV irradiation with H_2O_2, the magnetic biochar outperformed the unmodified biochar, particularly in terms of reaction rate and stability at higher dye concentrations, achieving a degradation efficiency of up to 98.85%. The novelty of this work lies in the valorization of an abundant, low-value banana peel waste into a magnetically recoverable photocatalyst whose overall greenness was quantitatively verified, yielding an AGREE score of 0.73. Beyond its scientific contribution to the design of biochar-based photocatalysts, the combination of waste valorization, minimal reagent consumption, and facile magnetic separation makes the system a practical and environmentally friendly candidate for the treatment of dye-containing wastewater.

REFERENCES

Alharbi, A.F., Alotaibi, A.A., Gomaa, H.E.M., Abahussain, A.A.M., Azeem, S.M.A., 2023. Magnetic Biochar by One-Step Impregnation Pyrolysis of Peganum harmala L . for Removal of Rhodamine B 2023. https://doi.org/10.1155/2023/9993465

Damertey, D., Nguyen, H., Ohemeng-boahen, G., Han, S., 2020. Science of the Total Environment Facile magnetic biochar production route with new goethite nanoparticle precursor. Science of the Total Environment 717, 137091. https://doi.org/10.1016/j.scitotenv.2020.137091

Deviliana, A., Nugroho, F.L., Rusmaya, D., 2019. Penyisihan Zat Warna Reactive Yellow 4R Oleh Fly Ash Yang Diaktivasi Secara Alkali Hidrotermal. Jurnal Unpas.

Elnour, A.Y., Alghyamah, A.A., Shaikh, H.M., Poulose, A.M., Al-zahrani, S.M., Anis, A., Al-wabel, M.I., 2019. applied sciences Effect of Pyrolysis Temperature on Biochar

Microstructural Evolution , Physicochemical Characteristics , and Its Influence on Biochar / Polypropylene Composites. Applied Sciences (Switzerland) 9, 7–9. https://doi.org/10.3390/app9061149

Fatimah, I., Purwiandono, G., Sahroni, I., Wijayana, A., Faraswati, M., Dwi Putri, A., Oh, W.C., Doong, R. an, 2022. Magnetically-separable photocatalyst of magnetic biochar from snake fruit peel for rhodamine B photooxidation. Environmental Nanotechnology, Monitoring and Management 17, 100669. https://doi.org/10.1016/j.enmm.2022.100669

Frankel, E.N., 2012. Photooxidation of unsaturated fats. Lipid Oxidation 51–66. https://doi.org/10.1533/9780857097927.51

Haryono, Faizal, M., Liamita, C., Rostika, A., 2018. Pengolahan Limbah Zat warna Tekstil Terdispersi Dengan Metode Elektroflotasi. EduChemia (Jurnal Kimia dan Pendidikan) 3, 94–105.

Hussain, Shabeeb, Hussain, Shazia, Waleed, A., Tavakoli, M.M., Wang, Z., 2016. Shabeeb Hussain, Shazia Hussain, Aashir Waleed, Mohammad Mahdi Tavakoli, Zilong Wang, Shihe Yang, Zhiyong Fan, Muhammad Arif Nadeem. ACS Applied Materials and Interfaces 8, 12460. https://doi.org/10.1021/acsami.6b12460

Irwan, Wayuningsih, Natsir, M., 2023. DEGRADASI LIGNIN DARI AMPAS SAGU MENGGUNAKAN FOTOKATALIS TiO2 DAN UJI AKTIFITAS ANTIBAKTERI. Jurnal Salome: Multidisipliner Keilmuan 1, 114–120.

Juliani, A., Rahmawati, S., Yoneda, M., 2021. Heavy Metal Characteristics of Wastewater From Batik Industry in Yogyakarta Area, Indonesia. International Journal of GEOMATE 20, 59–67. https://doi.org/10.21660/2021.80.6271

Kumar Mishra, R., Jaya Prasanna Kumar, D., Narula, A., Minnat Chistie, S., Ullhas Naik, S., 2023. Production and beneficial impact of biochar for environmental application: A review on types of feedstocks, chemical compositions, operating parameters, techno-economic study, and life cycle assessment. Fuel 343, 127968. https://doi.org/10.1016/j.fuel.2023.127968

Li, X., Qin, Y., Jia, Y., Li, Y., Zhao, Y., Pan, Y., Sun, J., 2021. Preparation and application of Fe/biochar (Fe-BC) catalysts in wastewater treatment: A review. Chemosphere 274, 129766. https://doi.org/10.1016/j.chemosphere.2021.129766

Navarathna, C.M., Dewage, N.B., Karunanayake, A.G., Farmer, E.L., Perez, F., Hassan, E.B., Mlsna, T.E., Pittman, C.U., 2020. Rhodamine B Adsorptive Removal and Photocatalytic Degradation on MIL-53-Fe MOF/Magnetic Magnetite/Biochar Composites. Journal of Inorganic and Organometallic Polymers and Materials 30, 214–229. https://doi.org/10.1007/s10904-019-01322-w

Ozkan, E., Ozturk, B., Karaaslan, M., Bay, M., Ay, S.B., Perkgoz, N.K., Palabıyık, İ.M., 2025. Green Synthesis and Characterization of Iron Oxide Nanoparticles Using Aronia. Cumhuriyet Science Journal 46, 457–463.

Pena-pereira, F., Wojnowski, W., Tobiszewski, M., 2020. AGREE Analytical GREEnness Metric Approach and Software. Analytical Chemistry 92, 10076−10082. https://doi.org/10.1021/acs.analchem.0c01887

Priyadarshini, M., Das, I., Ghangrekar, M.M., Blaney, L., 2022. Advanced oxidation processes: Performance, advantages, and scale-up of emerging technologies. Journal of Environmental Management 316, 115295. https://doi.org/10.1016/j.jenvman.2022.115295

Rafique, M., Shafiq, F., Ali Gillani, S.S., Shakil, M., Tahir, M.B., Sadaf, I., 2020. Eco-friendly green and biosynthesis of copper oxide nanoparticles using Citrofortunella microcarpa leaves extract for efficient photocatalytic degradation of Rhodamin B dye form textile wastewater. Optik 208, 1–8. https://doi.org/10.1016/j.ijleo.2019.164053

Reza, S., Afroze, S., Bakar, M.S.A., Saidur, R., Aslfattahi, N., 2020. Biochar characterization of invasive Pennisetum purpureum grass : effect of pyrolysis temperature. Biochar. https://doi.org/10.1007/s42773-020-00048-0

Rohayati, Z., Fajrin, M.M., Rua, J., Yulan, Y., Riyanto, R., 2017. Pengolahan Limbah Industri Tekstil Berbasis Green Technology Menggunakan Metode Gabungan Elektrodegradasi dan Elektrodekolorisasi dalam Satu Sel Elektrolisis. Chimica et Natura Acta 5, 95. https://doi.org/10.24198/cna.v5.n2.14702

Xie, Y., Wang, L., Li, H., Westholm, L.J., Carvalho, L., Thorin, E., Yu, Z., Yu, X., Skreiberg, Ø., 2022. A critical review on production, modification and utilization of biochar. Journal of Analytical and Applied Pyrolysis 161, 105405. https://doi.org/10.1016/j.jaap.2021.105405

Zakaria, N., Rohani, R., Wan Mohtar, W.H.M., Purwadi, R., Sumampouw, G.A., Indarto, A., 2023. Batik Effluent Treatment and Decolorization—A Review. Water 15. https://doi.org/10.3390/w15071339

Zhang, Y., Joel, M.Z., He, Y., Weathersby, D., Han, F., Rimal, G., Tang, J., Dai, Q., 2019. Materials Letters : X Synthesis of Fe 2 O 3 / biochar nanocomposites by microwave method for magnetic energy-storage concentration cells. Materials Letters: X 3, 100020. https://doi.org/10.1016/j.mlblux.2019.100020